LONGSHORE SEDIMENT TRANSPORT ON MEDITERRANEAN COAST OF ISRAEL

By Alexander Perlin[1] and Eliezer Kit[2]

ABSTRACT: A modified version of the CERC formula, which relates longshore sediment drift to deep water wave height and direction, has been used to define the equivalent wave height. The directional distribution of these wave heights and corresponding sediment transport rates and their analytical approximations are found using statistical analysis of high quality directional wave data measured simultaneously at two sites, Ashdod and Haifa. The directional distributions enable one to determine the directional shift between the average wave directions at both sites and to find the necessary corrections of wave directions at any location along the coast. The results emphasize the importance of accounting for wave directional shift in sediment transport calculations even when the locations are close. A detailed computation of directional shift for different ranges of wave heights is performed using correlation analysis of data sets. The corrections of wave directions at various locations along the coast are found by interpolation, and an excellent agreement between sediment fluxes at each location has been obtained when using the LITPACK package for littoral transport simulations with each data set.

INTRODUCTION

Longshore sediment transport is an important factor in shoreline change in response to the presence of marine structures, and, because of its practical engineering importance, it is treated and described in numerous monographs (e.g., Komar 1983; Sleath 1984; Bird 1985; Koutitas 1988; Rijn 1988; Fredsoe and Deigaard 1992; Nielsen 1992; Silvester and Hsu 1993). The idea that longshore sediment is mainly driven by waves rather than tides and ocean currents became generally accepted in the early twentieth century, and a formula relating the longshore sediment transport rate to the height and direction of the waves was first proposed by Munch-Petersen in 1938 (see Fredsoe and Deigaard 1992). Munch-Petersen's formula can be considered a forerunner of the Coastal Engineering Research Center (CERC) formula (*Shore* 1984).

Recently, more complicated models for sediment transport calculations have been developed that analyze in detail waves and corresponding radiation stress fields. This enables one to determine the longshore current and the distribution of sediment concentration in the vertical direction and then to find the sediment transport and the concurrent morphological changes. The description of such a model is given in Fredsoe and Deigaard (1992), and its implementation is made in an advanced LITPACK package developed by the Danish Hydraulic Institute (DHI), which is widely used in the current work.

The advantage of the CERC formula is that, due to its simplicity, it enables one to integrate contributions of waves arriving from various directions and to obtain an analytical expression for evaluation of sediment transport rate variations. The last are caused by changes of the mutual orientations of waves and the shorelines at different locations along the Mediterranean coast of Israel. Goldsmid and Golik (1980), Bird (1985), and Carmel et al. (1985) describe general characteristics of Israeli beaches. It is well known that this coast is part of the Nile Littoral Cell, where the source of sediments is the Nile Delta. With the exception of Mount Carmel, which protrudes into the sea forming Haifa Bay, the coastline is generally smooth with a gentle curvature expressed in the gradual change in orientation from N07°E in the north near the Carmel Head (Atlit North/Haifa South) to N36°E in the south near Ashkelon. Knowledge of the morphological regime and the net sediment transport in Ashkelon area is essential, because it determines the sediment flux entering the Mediterranean coast of Israel.

In the current work, estimates of sediment transport rates, employing an analytic expression based on the CERC formula, are obtained for the Israeli coast and are compared with the results of numerical simulations using the LITPACK model. The results of this section prove the importance of the correct determination of wave direction. In the next section, a statistical and correlation analysis of Ashdod and Haifa wave data is carried out to determine the directional shift for different wave height bands. Fine tuning of the wave directional shifts is carried out by applying the LITPACK package for sediment transport calculations. The corrected wave climate, including wave heights and directions, along the Israeli coast has thus been found. The sediment transport rates computed at any location, using each corrected data set (Haifa and Ashdod), are in excellent agreement within a few percent. It is worth noting that, without these corrections, the annual net sediment transport at some locations can even be in the opposite direction when compared with computations based on the original wave data.

WAVE DATA

In the present work, wave data sets measured simultaneously at two different sites, Ashdod and Haifa were used. The measurements were made by the Coastal and Marine Engineering Research Institute (CAMERI) on behalf of the Israeli Port and Railway Authority. At both sites, a Datawell Directional Buoy (Waverider) is deployed to acquire 30-minute records of surface elevation and directional spectral information. Generally, these records were acquired once each 3 hours, but during severe storm events, an attempt was made to collect data each hour. In the current work, only the limited information concerning the time series of significant wave height, wave period, and direction of wave propagation corresponding to the spectral peak is used. For simplicity, only the data points corresponding to the 3-hour time increment are selected. The data coverage is generally excellent, and, in the few cases of data gaps, an interpolation has been used to fill the gaps. The level of uncertainty in determination of the wave direction,

[1]PhD Student, Dept. of Fluid Mech. and Heat Transfer, Tel-Aviv Univ., Ramat-Aviv 69978, Israel.

[2]Prof., Dept. of Fluid Mech. and Heat Transfer, Tel-Aviv Univ., Ramat-Aviv 69978, Israel.

Note. Discussion open until September 1, 1999. To extend the closing date one month, a written request must be filed with the ASCE Manager of Journals. The manuscript for this paper was submitted for review and possible publication on August 27, 1998. This paper is part of the ***Journal of Waterway, Port, Coastal, and Ocean Engineering***, Vol. 125, No. 2, March/April, 1999. ©ASCE, ISSN 0733-950X/99/0002-0080–0087/ $8.00 + $.50 per page. Paper No. 19129.

due to the limited amount of information used for its evaluation, is relatively high—about ±5°. This uncertainty is caused by random errors. Therefore, it can be expected that, during the integration of the wave data (e.g., in sedimentological calculations), these errors will cancel out. The data set for Ashdod starts in April 1992 and the set for Haifa begins in December 1993. Three years of overlapping data, from April 1994 until April 1997, are used in the current work.

The annual wave data have been divided in two seasons: ''summer,'' which includes the seven months from April to October, and ''winter,'' which includes the five months from November to March. In summer, the wave field is usually calm, the wave height rarely exceeding 1–1.5 m, and the waves arrive on average from the west-northwest (WNW) direction. In winter, the frequency of storms is much higher and they are stronger than summer storms, but, at the same time, intervals of almost completely calm water are observed.

CERC FORMULA AND ITS INTEGRATION FOR WAVE STATISTICS

The CERC formula assumes a linear relationship between the longshore component of wave energy flux P_l entering the surf zone and the immersed weight of sand moved I_l:

$$I_l = KP_l \tag{1}$$

where K is a dimensionless coefficient.

The approximation for P_l at the breaker line, where celerity $C_b = C_g$ (the subscript b indicates values at the breaker line), is

$$P_{lb} = \frac{\rho g}{8} H_b^2 C_b \cos\theta_b \sin\theta_b \tag{2}$$

where H_b = wave height at breaking; and θ_b = wave direction at breaking. The submerged weight of sediment transport can be expressed as

$$I_l = \rho(s - 1)gQ \tag{3}$$

where Q = longshore sediment transport rate measured as solid volume; and s = relative density of sediment. It follows from the field measurements that the dimensionless coefficient K = 0.39 [e.g., *Shore* (1984), Komar and Inman (1970)] when a significant wave height appears in (2).

A useful form of the CERC formula that relates longshore sediment drift to deep water wave height and direction is given in Koutitas (1988) as

$$Q = 0.014 H_0^2 C_b \sin\theta_0 \cos\theta_0 \tag{4}$$

where H_0 = deep water significant wave height; and θ_0 = deep water wave angle. The empirical coefficient in (4) corresponds approximately to the value of 0.39 used in the original CERC formula. Using simplifying assumptions and empirical relations for breaking waves, Koutitas (1988) obtains an approximate expression for celerity of

$$C_b \approx 4H_0^{1/2} \quad \text{(in SI units)} \tag{5}$$

It follows from (4) and (5) that

$$Q = kH_0^{5/2} \sin 2\theta_0 \tag{6}$$

where $k \approx 0.028$. It is obvious that the value of the empirical constant k is site dependent and, perhaps, is a function of sand grain size. Nevertheless, there are indications in the different sources that this empirical coefficient is only weakly affected by grain size, the so-called CERC formula paradox (Nielsen 1988, 1992). Kamphius (1990) confirmed the weak grain size dependence.

Using further simplifying assumptions about the directional distribution of waves, the last formula can be integrated for all wave directions. Thus, an analytic expression can be obtained for the integrated sediment transport as a function of the relative shift between the equivalent mean wave direction and the shoreline orientation.

All waves in each time series are divided into 5° slots. The directional distribution function $p(\theta)$ presents the ratio of number of waves in the selected slot, N_θ, to the total number of waves, N. Waves with various heights in any slot can be represented by an equivalent wave height computed in accordance with the chosen way of averaging. The simplest equivalent wave height is the mean wave height:

$$H_{\text{av}} = \frac{1}{N_\theta} \sum_1^{N_\theta} H_i \text{ (first moment)}$$

The wave energy is presented by the root mean square wave height:

$$H_{\text{rms}} = \sqrt{\frac{1}{N_\theta} \sum_1^{N_\theta} H_i^2} \text{ (second moment)}$$

In accordance with (6), the equivalent wave height can be defined as

$$H_{\text{eq}} = \left(\frac{1}{N_\theta} \sum_1^{N_\theta} H_i^{5/2} \right)^{2/5}$$

Following this definition, the N_θ waves of the equivalent height H_{eq} produce the same sediment transport as all waves entering the 5° slot. Figs. 1(a and b) represent for Ashdod and Haifa, respectively, the directional distributions of equivalent wave heights H_{eq} together with the average heights H_{av} and the root mean square heights H_{rms}.

The second important parameter—the wave probability distribution $p(\theta)$—is shown in Figs. 1(c and d) along with the equivalent wave height H_{eq}. These two parameters allow one to calculate the annual longshore transport:

$$Q = 3{,}600 \cdot 24 \cdot 365 \cdot \frac{180}{5\pi} \int kp(\theta) H_{\text{eq}}^{5/2}(\theta) \sin 2(\theta_s - \theta)\, d\theta \tag{7}$$

where θ = direction of wave vector; and θ_s = direction of the normal to the shoreline, relative to the north, at the chosen location.

The product $f(\theta) = p(\theta) H_{\text{eq}}^{5/2}(\theta)$, which expresses the contribution of waves coming from the chosen direction to the sediment transport, is presented in Figs. 1(c and d) for Ashdod and Haifa. The shape of the plots enables one to use the Gaussian distribution for fitting [Figs. 1(e and f) for Ashdod and Haifa, respectively]:

$$f(\theta) = A/w\sqrt{\pi/2} \exp -2((\theta - \bar{\theta})/w)^2 \tag{8}$$

The three free parameters in (8)—A, w, and $\bar{\theta}$—can be computed using the least squares fit to the data. The parameter A determines the area of distribution function; w indicates the width of the distribution; and $\bar{\theta}$ = mean wave direction in a selected set of data and shows the shift of the center of the distribution function $f(\theta)$ relative to the north. Because the shape of the Haifa wave data is more complicated and there are indications for two peaks in the distribution function, the parameters A and w computed for Ashdod have also been used to evaluate the mean wave direction $\bar{\theta}$ for the Haifa set. At first glance, the last plot [Fig. 1(f)] represents even better the higher values of wave data. However, the slightly lower value of A for Ashdod, when used for the Haifa set, can lead to lower values of the sediment transport rate computed with the Haifa set of wave data. The computed parameters for the Ashdod and Haifa data sets are shown in the second and third columns of Table 1. The additional set of parameters for Haifa

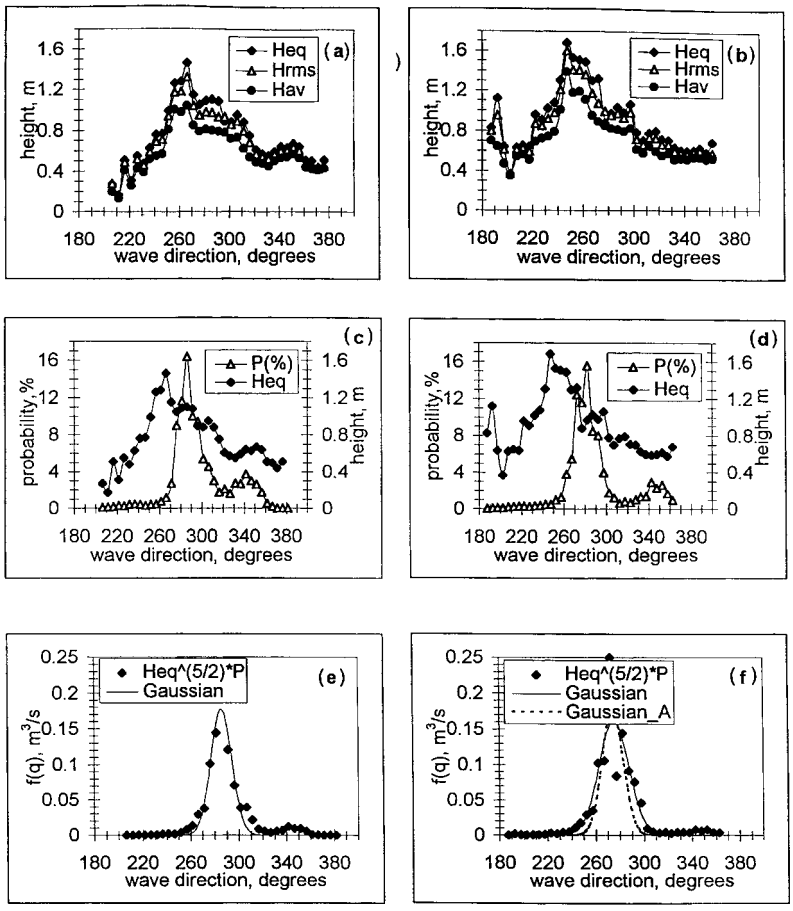

FIG. 1. Directional Distribution of Field Wave: (a), (b) Various Equivalent Wave Heights for Ashdod and Haifa Data Sets, Respectively; (c), (d) Directional Probability of Waves in Selected Slot $p(\theta)$ for Ashdod and Haifa, Respectively; (e), (f) Least Square Fit of Product $(H_{eq})^{5/2}$ $p(\theta)$ for Ashdod and Haifa, Respectively

TABLE 1. Parameters of Directional Wave Distribution Function Computed by Applying Nonlinear Least Square Gaussian Fit

Parameter (1)	Ashdod (2)	Haifa (3)	Haifa A (4)
A	0.067	0.088	0.067
w	0.30	0.43	0.30
$\bar{\theta}$ (rad)	4.99	4.80	4.79
$\bar{\theta}$ (degrees)	285.6	275.2	274.3
$A \cdot \exp(-w^2/2)$	0.064	0.080	0.064
SSR	0.004	0.016	0.022

Note: SSR = square sum of residuals.

is determined, as mentioned above, by the best fit of the Haifa wave data while using the A and w values that have been computed for Ashdod. It follows from the plots and from Table 1 that the mean wave direction deviates in Haifa from that in Ashdod, the difference for the two wave sets being at least 10.5°. This directional shift is the same for all waves in a set, independently of their height. The influence of different ranges of wave heights on the directional shift will be discussed in the next section. It follows from Fig. 1 and Table 1 that, on average, the waves in Haifa are slightly higher than those in Ashdod. This difference is small but noticeable.

Using the best fit of $f(\theta)$ and (7), the following expression for annual sediment rate Q in cubic meters per year is obtained:

$$Q = 3{,}600 \cdot 24 \cdot 365 \cdot \frac{180}{5\pi} kA \int \frac{1}{w\sqrt{\pi/2}} \exp((\theta - \bar{\theta})/w)^2 \cdot \sin 2(\theta_s - \theta)\, d\theta \quad (9)$$

Actually, the wave angle θ varies between $\pi/2 - \theta_s$ and $\pi/2 + \theta_s$, but, because the Gaussian function decays very fast and vanishes at the bounds, the integral I can be rewritten as following, and its value can be found in Gradshteyn and Ryzhik (1980):

$$I = \int_{-\infty}^{\infty} \frac{1}{w\sqrt{\pi/2}} \exp((\theta - \bar{\theta})/w)^2 \sin 2(\theta_s - \theta)\, d\theta = e^{-w^2/2} \sin 2(\theta_s - \bar{\theta}) \quad (10)$$

Hence, the net transport is equal to

$$Q = I \cdot k \cdot A \cdot 3{,}600 \cdot 24 \cdot 365 \cdot \frac{180}{5\pi} = 101 \cdot 10^5 \cdot A \cdot e^{-w^2/2} \cdot \sin 2(\theta_s - \bar{\theta}) \quad (11)$$

The analytical expression (11) shows that the functional dependence of the net sediment flux on the mean wave direction $\bar{\theta}$ is essential. For small values $(\theta_s - \bar{\theta})$, which usually occur along the Israeli coast from Ashdod to Haifa, the net sediment flux is proportional to this difference. From Ashdod to Haifa South, where the beach is still sandy, the azimuth θ_s varies from 295° at Ashdod to 277° at Haifa South. It follows that (11) will result in a very strong southern net sediment flux in Haifa South when the Ashdod set of data is used, because $(\theta_s - \bar{\theta})$ is negative. The more appropriate Haifa data set leads to a northern transport. The preliminary computations of net sediment transport rate as a function of coast orientation θ_s, using (11) and wave parameters from the Ashdod and Haifa data sets, are shown in Fig. 2(a). Also shown in this figure is a plot of sediment transport simulations using the LITPACK package with the Ashdod wave data set. The details of the last

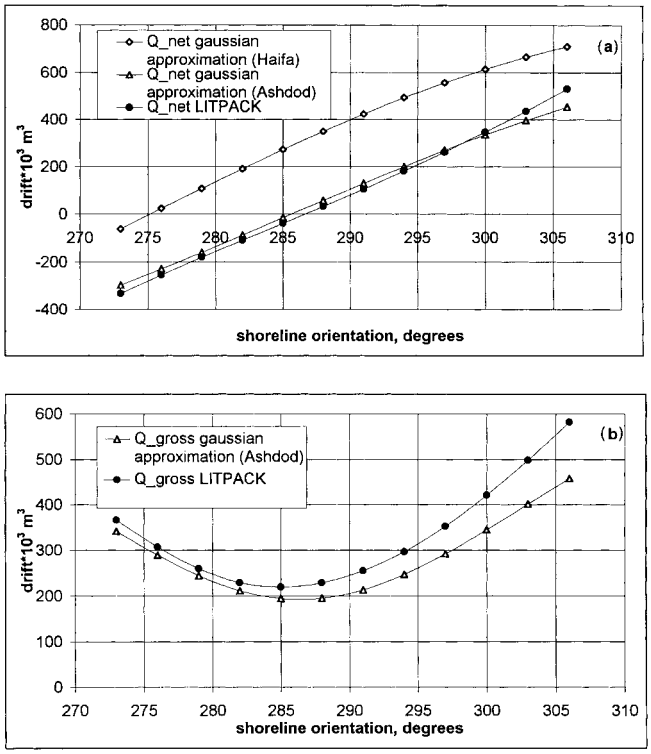

FIG. 2. Annual Sediment Transport Rates Computed Applying CERC Formula and LITPACK Package at Various Shoreline Orientations: (a) Net Flux; (b) Gross Transport (No Corrections of Wave Data Sets Employed)

computation will be discussed later, as, for the moment, the writers wish only to stress the striking resemblance of the two plots, which are obtained by two essentially different approaches. In Fig. 2(b), the annual gross sediment transport rate is shown, which comprises the absolute values of the northern and southern sediment fluxes. It should be clarified that an analytic expression cannot be derived for the gross transport, and the integral in (10) was computed numerically for both northern and southern fluxes. It is obvious that, for sediment transport computations at any location, there is a need for determination of the mean wave direction $\bar{\theta}$ at the location. The simplest assumption is that it varies linearly between Haifa and Ashdod and, hence, can be found by applying linear interpolation.

DIRECTIONAL SHIFT

As mentioned previously, the values of wave directions along the Israeli coast could be obtained by interpolation of the directional shift between mean wave directions at the Haifa and Ashdod sites. However, such an approach assumes that the directions of all waves are shifted by the same angle. Let us first discuss the underlying physics leading to the directional shift.

The main assumption is that storm events are related to areas or storm ''centers,'' and the waves propagating from these areas towards the coast are highly coherent (see the sketch in Fig. 3). The directional shift following from this assumption and that reported in the previous section have the same sign. It can also be easily seen that, if the distance from the storm center to the coast is significantly larger than the distance between Ashdod and Haifa sites, the use of linear interpolation for determination of the directional shift for any other location along the coast is appropriate. This assumption is not suitable for small waves, say, less than 0.5 m because their generation is mostly related to the local winds and coherency of waves cannot be expected. For these waves, the directional shift between different locations along the coast can be of any sign. When the wave height increases, the coherency of the waves at different sites along the coast should increase and a directional shift must be sensed. The bigger waves are naturally related to larger fetches and to greater distances from the coast. It is obvious from Fig. 3 that increasing the distance between the storm area and the specific site leads to a decrease in the directional shift. It follows from these considerations that, on one hand, the coherency of the waves improves for far-off sources and, concurrently, the directional shift becomes more definite, while, on the other hand, its value decreases with the distance of the storm center from the site. These opposite trends should lead to directional shifts of practically zero for the lowest and highest waves, and to nonmonotonous behavior of the directional shift in the whole range of wave heights.

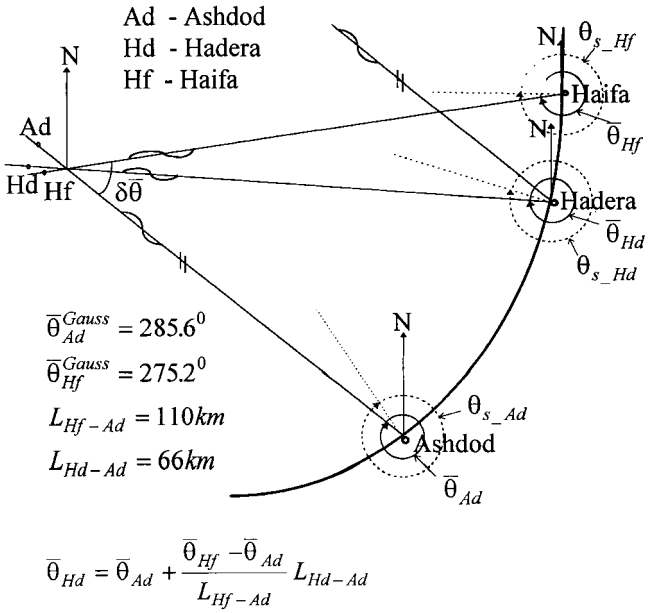

FIG. 3. Sketch of Waves Propagation from Storm Center towards Various Sites of Mediterranean Coast of Israel

To verify these assumptions and to determine the actual directional shift of the waves, a correlation analysis was carried out between the waves in both sets (Haifa and Ashdod). All waves in the Ashdod set are divided into slots according to wave height increments of 0.5 m. Because of the small number of waves greater than 3 m, all such waves are treated as being in one slot. The corresponding slots of wave heights and directions in the Haifa wave data set are obtained in consonance to the time of measurements. The mean values and standard deviations of wave heights and directions in each slot of each one of data sets and their correlation for both data sets are computed according to following expressions:

$$\bar{x} = \frac{1}{n}\sum_{i=1}^{n} x_i,\ \bar{y} = \frac{1}{n}\sum_{i=1}^{n} y_i \tag{12a}$$

$$m_{2x} = \frac{1}{n}\sum_{i=1}^{n} (x_i - \bar{x})^2 = \frac{1}{n}\sum_{i=1}^{n} x_i^2 - \bar{x}^2 \tag{12b}$$

$$m_{2y} = \frac{1}{n}\sum_{i=1}^{n} (y_i - \bar{y})^2 = \frac{1}{n}\sum_{i=1}^{n} y_i^2 - \bar{y}^2 \tag{12c}$$

$$m_{xy} = \frac{1}{n}\sum_{i=1}^{n} (x_i - \bar{x})(y_i - \bar{y}) = \frac{1}{n}\sum_{i=1}^{n} x_i y_i - \overline{xy} \tag{12d}$$

$$r = \frac{m_{xy}}{\sqrt{m_{2x} m_{2y}}} \tag{12e}$$

where m_{2x} and m_{2y} = mean square deviation of the wave height/direction distribution in Ashdod and Haifa, respectively; m_{xy} = covariance of two variables; and r = correlation coefficient. In the above expressions, x denotes the wave height or direction of the Ashdod data set and y is used for the Haifa data set. The computation has been performed for each slot separately; the directional shift for each wave height range (slot) is defined as $\delta\theta = \theta_{\text{Ashdod}} - \theta_{\text{Haifa}}$ and wave height ratio as $R_H = H_{\text{Haifa}}/H_{\text{Ashdod}}$, where mean wave heights and directions computed for each slot (12*a*) are used. As mentioned above, this analysis is performed for the following wave height slots: 0–0.5, 0.5–1.0, 1.0–1.5, 1.5–2.0, 2.0–2.5, 2.5–3.0, and >3.0 m. The correlation coefficient for wave heights r_H and wave height ratio R_H, and the correlation coefficient for wave directions r_θ and directional shift $\delta\theta$ are presented in Tables 2 and 3, respectively. To account for the possible delay of waves arriving from a storm center to one of the sites (Ashdod or Haifa), the calculations are carried out with various time lags. Due to the nature of the data, the time lag can be only an integer number with a minimal increment of 3 hours.

The results of Table 2 confirm the expected nonmonotonic behavior of the wave height correlation coefficient and show again that waves at the Haifa site are somewhat higher (on the average, $R_H = 1.08$) than those in Ashdod. A similar result was already noted in the previous section.

The results presented in Table 3 also confirm the nonmonotonous behavior of directional correlation as a function of wave height ranges. The negative directional shift at the lowest range of wave height 0.0–0.5 m can be explained by the somewhat different structure of local winds at two sites. In the second range, 0.5–1.0 m, the correlation is still very low, but the directional shift has a correct sign, indicating that, in part, the waves are arriving from a common coherent source and, mostly, are generated by the local wind. The correlation reaches high values, exceeding 0.8, in the third region and then falls down again. The minimum value of correlation and the relatively low value of directional shift in the region 2–2.5 m indicate some balance between wave generation by coherent source and local wind. The directional shift and correlation increase with a further increase of the wave height. There is not enough data for detailed analysis of waves significantly higher than 3 m, for which directional shift can be expected to decrease. The results of Tables 2 and 3 show also that the suggested physical picture is oversimplified and, though it captures the main features, the real phenomenon is more complicated. Nevertheless, the results of Table 3 represent a good basis for wave directional shift computations along the Mediterranean coast of Israel, and so they are used in the subsequent numerical simulations.

LITTORAL DRIFT CALCULATIONS AT DIFFERENT SITES ALONG COAST

Computations of longshore sediment transport rates at various sites along the Israeli coast, from Ashkelon to Haifa, have been performed employing the LITPACK package. The simulations are carried out with both wave data sets (Ashdod and Haifa) using the directional shifts for each wave height range as determined in the previous section.

LITPACK is an advanced package for literal sediment transport computations, which uses a sophisticated approach involving wave radiation stress computations for evaluation of longshore sediment flux. The longshore transport rate Q is calculated using one-dimensional momentum equations for both velocity components and the turbulent diffusion equation for sediment concentration. The driving force in the momentum equations is the radiation stress induced by wave breaking. A detailed description of the approach can be found in Fredsoe and Deigaard (1992). The limitation of the package is that it is most suitable for two-dimensional beaches with parallel depth contours. The model requires knowledge of the mean grain diameter d_{50} and of the sediment spreading, $\sigma_g = \sqrt{d_{84}/d_{16}}$, and it does not put any constraints on the shape of the bottom profile.

The bottom profile at a remote (in respect to marine structures) cross section was chosen for the simulations (Kit and Pelinovsky 1998). It is worth noting that variations of the bottom profile and the median size of sand grains along the coast

TABLE 2. Wave Height Correlation and Ratio

Height range (m) (1)	r_h at Time Delays in Hours of					R_h at Time Delays in Hours of				
	−6 (2)	−3 (3)	0 (4)	3 (5)	6 (6)	−6 (7)	−3 (8)	0 (9)	3 (10)	6 (11)
$0.0 \le H \le 0.5$	0.14	0.15	0.15	0.14	0.11	1.10	1.10	1.09	1.10	1.12
$0.5 \le H \le 1.0$	0.54	0.61	**0.64**	0.57	0.47	1.05	1.05	**1.04**	1.04	1.04
$1.0 < H \le 1.5$	0.36	0.46	**0.51**	0.44	0.36	1.03	1.05	**1.05**	1.04	1.03
$1.5 < H \le 2.0$	0.40	**0.49**	0.47	0.34	0.31	1.06	**1.08**	1.08	1.07	1.07
$2.0 < H \le 2.5$	0.23	0.24	**0.27**	0.15	0.08	1.06	1.08	**1.08**	1.06	1.04
$2.5 < H \le 3.0$	0.29	**0.35**	0.27	0.18	−0.02	1.05	**1.10**	1.09	1.06	1.03
$3.0 < H$	0.24	**0.42**	0.11	−0.05	−0.07	1.01	**1.06**	1.06	1.04	0.98

Note: Maximum correlation and corresponding wave height ratio are shown in bold numbers.

TABLE 3. Wave Directional Correlation and Shift

Height range (m) (1)	r_θ at Time Delays in Hours of					$\delta\theta$ at Time Delays in Hours of				
	−6 (2)	−3 (3)	0 (4)	3 (5)	6 (6)	−6 (7)	−3 (8)	0 (9)	3 (10)	6 (11)
$0.0 \le H \le 0.5$	0.32	0.35	0.38	0.39	0.37	−8.69	−8.68	−8.61	−8.30	−7.68
$0.5 \le H \le 1.0$	0.27	0.33	**0.36**	0.34	0.32	6.63	6.79	**6.97**	6.72	6.20
$1.0 \le H \le 1.5$	0.59	0.76	**0.82**	0.76	0.58	9.37	8.00	**7.63**	7.64	7.60
$1.5 < H \le 2.0$	0.61	**0.70**	0.66	0.64	0.61	10.03	**10.74**	10.29	10.00	9.85
$2.0 < H \le 2.5$	0.39	0.60	**0.62**	0.60	0.42	8.73	7.94	**7.89**	7.65	7.53
$2.5 < H \le 3.0$	0.47	0.53	**0.76**	0.67	0.52	13.22	12.00	**12.84**	11.69	11.61
$3.0 < H$	0.78	**0.84**	0.80	0.78	0.70	14.70	**14.83**	12.92	11.92	11.72

Note: Maximum correlation and corresponding directional shift are shown in bold numbers.

occur but are not dramatic. Values of $d_{50} = 180\mu$ and $\sigma_g = 1.4$ were chosen for use in the computations.

Computations of the annual net and gross sediment transport rates, carried out using the time series of the Ashdod data set for various coastal orientations, are given in Fig. 2. The gross sediment transport determines the morphodynamic activity of a specific region under the action of waves. It can be significant even in regions with zero net transport. Remarkably similar behavior can be noticed in Figs. 2(a and b) between results computed by the LITDRIFT module of the LITPACK package and by applying the modified CERC formula. The coast orientation, where the net transport vanishes and the gross transport has a minimum, corresponds to the integral mean wave direction. It follows from Fig. 2 that this direction is about 285°–286°, as predicted by the Gaussian presentation of the product $f(\theta) = p(\theta)H_{eq}^{5/2}(\theta)$ (Table 1).

These computations also enable one to separate the net and gross transport between summer and winter. The results for the Ashdod data set are shown in Fig. 4. As expected, the total annual transport practically coincides with that during the winter season, because the summer transport is very low. This result should be treated with care, because the sediment transport during the summer season might be important for computations in the vicinity of the marine structures.

Annual sediment transports of about 200,000 m^3 in the Ashdod area and more than 400,000 m^3 in the Ashkelon area (306°), are computed by two methods: (1) using an integral expression based on the CERC formula; and (2) from LITDRIFT module simulations. These figures seem to be plausible. In particular, the sand trapped by the Ashdod port, which is the biggest marine structure on the Israeli coast, provides similar estimates. It should be emphasized that the CERC formula has been used with the original coefficients and no additional assumptions were made except those suggested by Koutitas (1988) in order to relate the sediment transport to wave characteristics in the deep sea instead of at the breaking line.

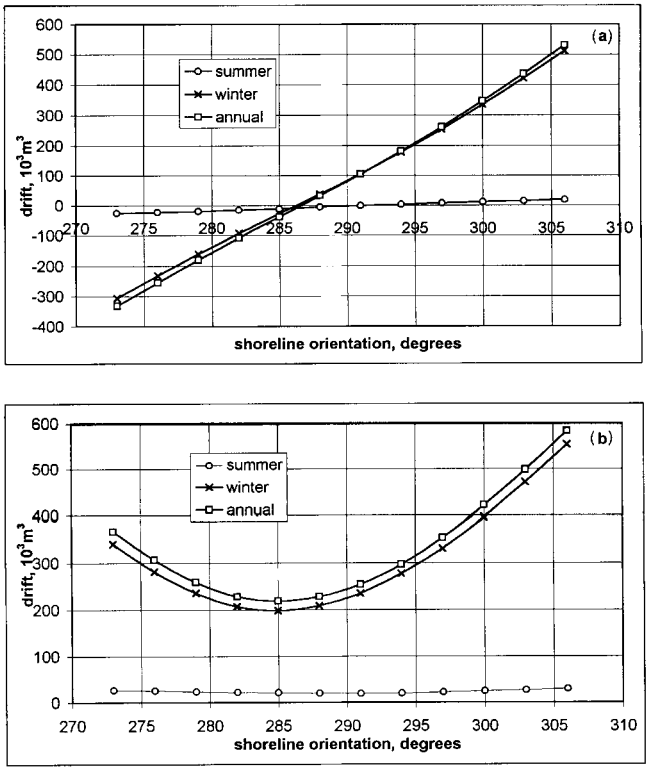

FIG. 4. Annual and Seasonal (Summer and Winter) Sediment Transport Rates Computed Applying LITPACK Package and Uncorrected Ashdod Wave Data Set at Various Shoreline Orientations: (a) Net Flux; (b) Gross Transport

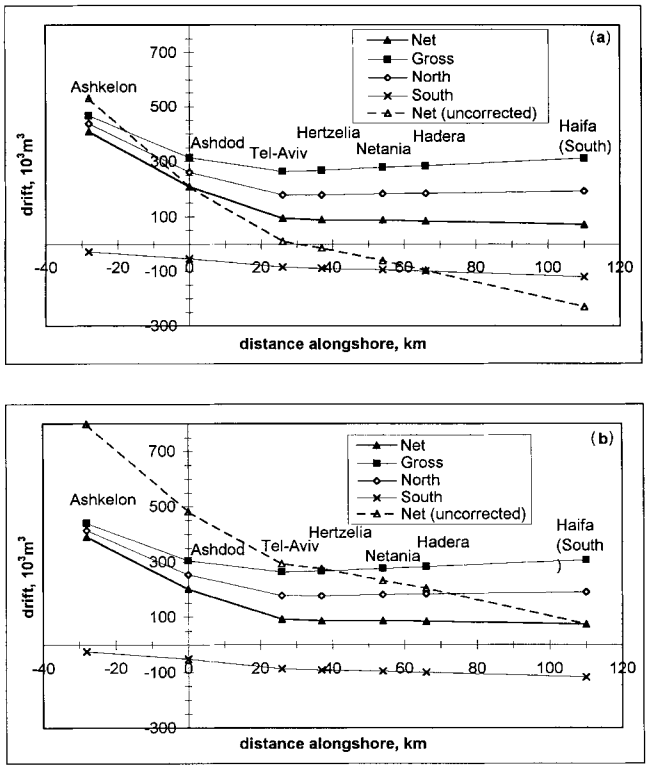

FIG. 5. Annual (Net, Gross, Northern, and Southern) Sediment Transport Rates Computed Applying LITPACK Package at Various Sites of Mediterranean Coast of Israel: (a) Ashdod Wave Data Set; (b) Haifa Wave Data Set (Directions and Wave Heights Corrected According to Table 4)

Computations of longshore sediment transport at different sites along the coast, from Ashkelon to Haifa, have been performed using both the Haifa and the Ashdod data sets. To correct the wave directions at each site, the directional shifts determined by correlation analysis in the previous section are applied. Linear interpolation is used to calculate the appropriate directional shift and the wave height ratio at various locations along the coast. It should be emphasized that the variations of the latter are very moderate; their whole range constitutes 8%. The agreement between computed rates of sediment fluxes applying both sets of wave data was very reasonable, but systematic trends were noticed; the sediment transport rate in Ashdod computed by employing the Haifa data set was somewhat greater than that obtained using the local Ashdod data, and vice versa. Therefore, an additional directional shift correlation of 1.5° for all wave heights has been made. The results of the computations of annual sediment fluxes are given in Fig. 5. There is practically no difference between the sediment fluxes computed employing the Ashdod [Fig. 5(a)] and the Haifa [Fig. 5(b)] data sets. On the other hand, when both sets of wave data are used without corrections, the uncorrect net transport, shown in Figs. 5(a and b), can differ even in sign at the same location. The necessary corrections of wave directions and wave heights for each of the data sets at various sites of the coast are given in Table 4. Thus, each of the data sets can be used for determination of the wave climate at any chosen location along the coast between Ashkelon and Haifa.

It is worth emphasizing the limitations of the procedures and the assumptions for which the wave data and the computations of the sediment transports are valid:

1. The wave data sets are limited in time (three years of

TABLE 4. Height and Wave Angle Corrections for Generation of Wave Climate at Particular Locations along Israeli Coast

Location (1)	θ_s-270° (2)	L (km) (3)	R_h (4)	δθ (deg) for Height Ranges of 0–0.5 (5)	0.5–1 (6)	1–1.5 (7)	1.5–2 (8)	2–2.5 (9)	2.5–3 (10)	>3 (11)
(*a*) Ashdod data set										
Ashkelon	36	−28	0.98	0	2.2	2.4	3.2	2.4	3.7	4.2
Ashdod	25	0	1.00	0	0	0	0	0	0	0
Tel-Aviv	17	26	1.02	0	−2.0	−2.2	−3.0	−2.2	−3.4	−3.9
Hertzelia	16	37	1.03	0	−2.9	−3.2	−4.2	−3.2	−4.9	−5.6
Netania	14	54	1.04	0	−4.2	−4.7	−6.1	−4.7	−7.1	−8.1
Hadera	12.5	66	1.05	0	−5.1	−5.7	−7.5	−5.7	−8.7	−9.9
Haifa	7	110	1.08	0	−8.5	−9.5	−12.5	−9.5	−14.5	−16.5
(*b*) Haifa data set										
Ashkelon	36	138	0.91	0	10.7	11.9	15.7	11.9	18.2	20.7
Ashdod	25	110	0.93	0	8.5	9.5	12.5	9.5	14.5	16.5
Tel-Aviv	17	84	0.94	0	6.5	7.3	9.5	7.3	11.1	12.6
Herzelia	16	73	0.95	0	5.6	6.3	8.3	6.3	9.6	11.0
Netania	14	56	0.96	0	4.3	4.8	6.4	4.8	7.4	8.4
Hadera	12.5	44	0.97	0	3.4	3.8	5.0	3.8	5.8	6.6
Haifa	7	0	1.00	0	0	0	0	0	0	0

Note: L = distance between locations and site where actual wave measurements have been performed.

overlapping data off the Ashdod and Haifa coasts). During these three years, unusually strong storm events did not occur. It would be advantageous to verify the results of the current work using more complete data sets when they eventually are acquired.

2. The computations of sediment transport are valid for regions where the beach is sandy, the bathymetry varies slowly, and the chosen cross section is far enough from marine structures and from regions where the shoreline orientation undergoes fast modifications. It is obvious that, in the latter regions, more advanced two- or three-dimensional models are necessary. Description and implementations of such models can be found in Watanabe et al. (1986) and de Vriend et al. (1993).

CONCLUDING REMARKS

The use of a modified CERC formula with an appropriate statistical distribution of wave directions in the deep water enabled the writers to derive an analytical expression for the annual net longshore sediment transport. This expression shows a very strong dependence of the sediment transport on a mutual orientation of a characteristic wave direction and shoreline azimuth. Sets of high-quality directional wave data measured at two different sites (Haifa and Ashdod), separated by 110 km along the coast of Israel, enabled us to estimate the correct characteristic wave directions at various sites. The current research demonstrates that the use of uncorrected wave directions based on a single data set can result in an erroneous calculated sediment transport and, for some locations, can lead even to a wrong direction for the net calculated sediment transport. It follows also from this work that only high quality wave directional data can be used to find the wave directional shift and to establish the necessary corrections at various sites. Although the integral directional shift for the whole wave data, found by applying the CERC formula, demonstrates a correct trend, the underlying physics indicates that the directional shift should be strongly affected by wave height and this dependence is nonmonotonous.

Therefore, the required corrections of wave directions and wave heights at various sites has been found by executing a thorough correlation analysis of both wave data sets that accounts for various ranges of wave heights. The sediment transport computations at different sites along the coast, carried out by employing an advanced LITPACK package and corresponding corrections of wave directions and wave heights, confirmed the validity of the suggested approach. A fine tuning of corrections of wave directions in both sets was sufficient to provide a perfect agreement of computed sediment fluxes at any location on the coast, using each wave data set. Thus, the wave climate can be established at any location along the Mediterranean coast of Israel, providing that it is known at one of the sites, for example, either at Haifa or at Ashdod.

Although the derivation of the analytic expression and the data analysis rely on directional wave data measured at a specific site on the Israeli coast, the conjectures from this work are expected to be common to other sites, because the underlying physics for wave directions' shift at various locations is of a general nature. The importance of accounting for this shift follows from the fact that it affects significantly the longshore sediment transport at various locations even of the relatively short Israeli coast.

ACKNOWLEDGMENTS

This work was supported by the Ministry of Science (Grant No. 6719-1-95). The permission to use wave data from the Israeli Port and Railway Authorities and the assistance of CAMERI researchers are highly appreciated.

APPENDIX I. REFERENCES

Bird, E. C. F. (1985). *Coastline changes: a global review.* Wiley, Chichester, U.K.

Carmel, Z., Inman, D., and Golik, A. (1985). ''Directional wave measurement at Haifa, Israel, and sediment transport along the Nile Littoral Cell.'' *Coast. Engrg.*, 9, 21–36.

De Vriend, H. J., Zyserman, J., Nicholson, J., Roelvink, J. A., Pechon, P., and Southgate, H. N. (1993). ''Medium-term 2DH coastal area modelling.'' *Coast. Engrg.*, 21, 193–224.

Fredsoe, J., and Deigaard, R. (1992). *Mechanics of coastal sediment transport: advanced series on ocean engineering.* World Science, Singapore.

Goldsmith, V., and Golik, A. (1980). ''Sediment transport model of the southeastern Mediterranean Coast.'' *Marine Geology*, 37, 147–175.

Gradshteyn, I. S., and Ryzhik, I. M. (1980). *Table of integrals, series, and products.* Academic, San Diego.

Kamphuis, J. W. (1990). ''Littoral transport rate.'' *Proc., 22nd Int. Conf. Coast. Engrg.*, ASCE, Reston, Va., 2402–2415.

Kit, E., and Pelinovsky, E. (1998). ''Dynamical models for cross-shore transport and equilibrium bottom profiles.'' *J. Wtrwy., Port, Coast., and Oc. Engrg.*, ASCE, 124(3), 138–146.

Komar, P. D., ed. (1983). *Handbook of coastal processes and erosion.* CRC Press, Boca Raton, Fla.

Komar, P. D., and Inman, D. L. (1970). ''Longshore sand transport on beaches.'' *J. Geophys. Res.*, 75(33), 5914–5927.

Koutitas, C. G. (1988). *Mathematical models in coastal engineering.* Pen tech Press, London.
Nielsen, P. (1988). ''Towards modeling coastal sediment transport.'' *Proc., 21st Int. Conf. on Coast. Engrg.*, ASCE, Reston, Va., 1952–1958.
Nielsen, P. (1992). *Coastal bottom boundary layers and sediment transport: Advanced series on ocean engineering.* World Scientific Publication, Singapore.
Rijn, L. C. (1988). *Handbook on sediment transport by currents and waves.* Delft Hydraulics, Delft, The Netherlands.
Shore protection manual. (1984). 4th Ed., Coast. Engrg. Res. Ctr., U.S. Army Corps of Engineers, Washington, D.C.
Silvester, R., and Hsu, J. R. C. (1993). *Coastal stabilization: innovative concepts.* Prentice-Hall, Englewood Cliffs, N.J.
Sleath, J. F. A. (1984). *Sea bed mechanics.* Wiley, New York.
Watanabe, A., Maruyama, K., Shimizu, T., and Sakakiyama, T. (1986). ''Numerical prediction model of three-dimensional beach deformation around a structure.'' *Coast. Engrg. in Japan*, Tokyo, 29, 179–194.

APPENDIX II. NOTATION

The following symbols are used in this paper:

A = area of distribution function;
C_b = phase velocity of waves at breaker line;
C_g = group velocity of waves;
d_{16}, d_{50}, d_{84} = grain size exceeding by weight 16%, 50%, and 84% of particles, respectively;
E = wave energy;
$f(\theta)$ = distribution function;
H = significant wave height;
$\bar{H}_{\text{Ashdod}}$, $\bar{H}_{\text{Haifa}}$ = mean wave height in Ashdod and Haifa, respectively;
H_{av} = mean wave height;
H_b = wave height at breaker line;
H_{eq} = equivalent wave height;
H_i = arbitrary wave height in time series;
H_{rms} = root mean square wave height;
H_0 = deep water significant wave height;
h_b = water depth at breaker line;
g = acceleration of gravity;
I = integral;
I_l = immersed weight of sand;
K = dimensionless coefficient;
k = empirical constant;
m_{xy} = covariance of two variables;
m_{2x} = mean square deviation of wave height/direction distribution in Ashdod;
m_{2y} = mean square deviation of wave height/direction distribution in Haifa;
N = total number of waves;
N_θ = number of waves in selected slot;
n = number of events in selected slot;
P = wave energy flux;
P_l = longshore component of wave energy flux;
P_{lb} = longshore component of wave energy flux at breaking line;
$p(\theta)$ = directional distribution function;
Q = longshore volumetric drift;
R_H = wave height ratio;
r = correlation coefficient;
r_H = correlation coefficient for wave heights;
r_θ = correlation coefficient for wave direction;
s = relative density of sediment;
w = width of distribution function;
x = wave height/direction in Ashdod;
y = wave height/direction in Haifa;
$\delta\theta$ = wave directional shift;
$\underline{\theta}$ = angle of wave crest with shoreline;
$\bar{\theta}$ = mean wave direction in distribution function;
θ_b = wave direction at breaker line;
θ_s = angle of normal to shoreline relative to north;
θ_0 = deep water wave direction;
ρ = water density; and
σ_g = sediment spreading.